Supporting Information

Photocatalytic CO_2 Reduction Using Metal Complexes in Various Ionic Liquids

Yoshiyuki Asai, Haruka Katsuragi, Kazuki Kita,
Taro Tsubomura and Yasuomi Yamazaki *

Department of Materials and Life Science, Seikei University, 3-3-1 Kichijoji-kitamachi,
Musashino-shi, Tokyo, 180-8633, Japan.

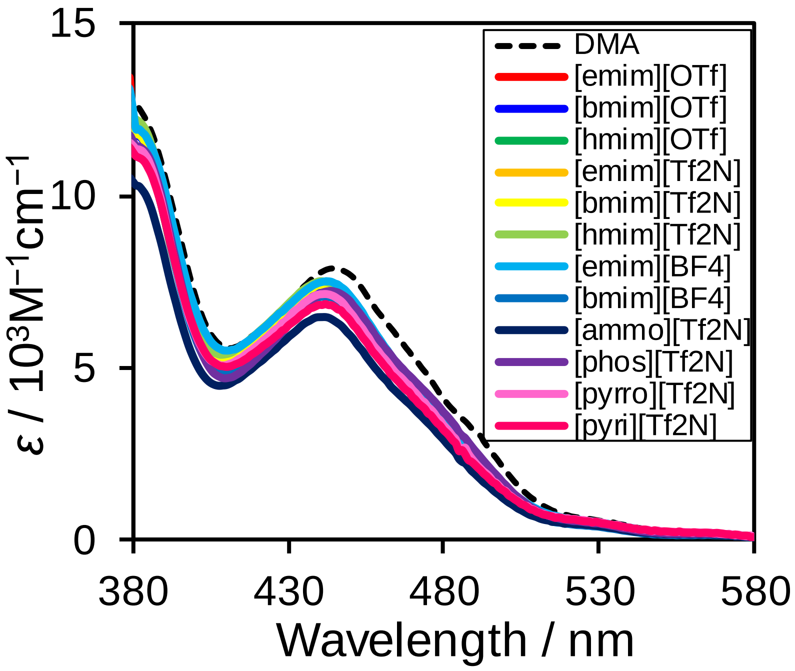

Figure S1. UV-Vis absorption spectra of **Ir** in each of the ionic liquids.

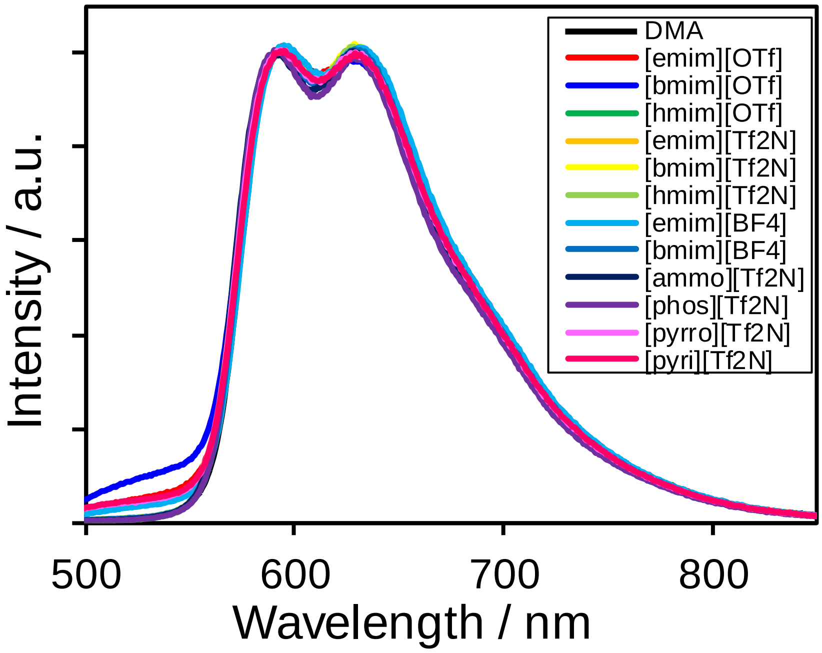

Figure S2. Emission spectra of **Ir** in each of the ionic liquids.

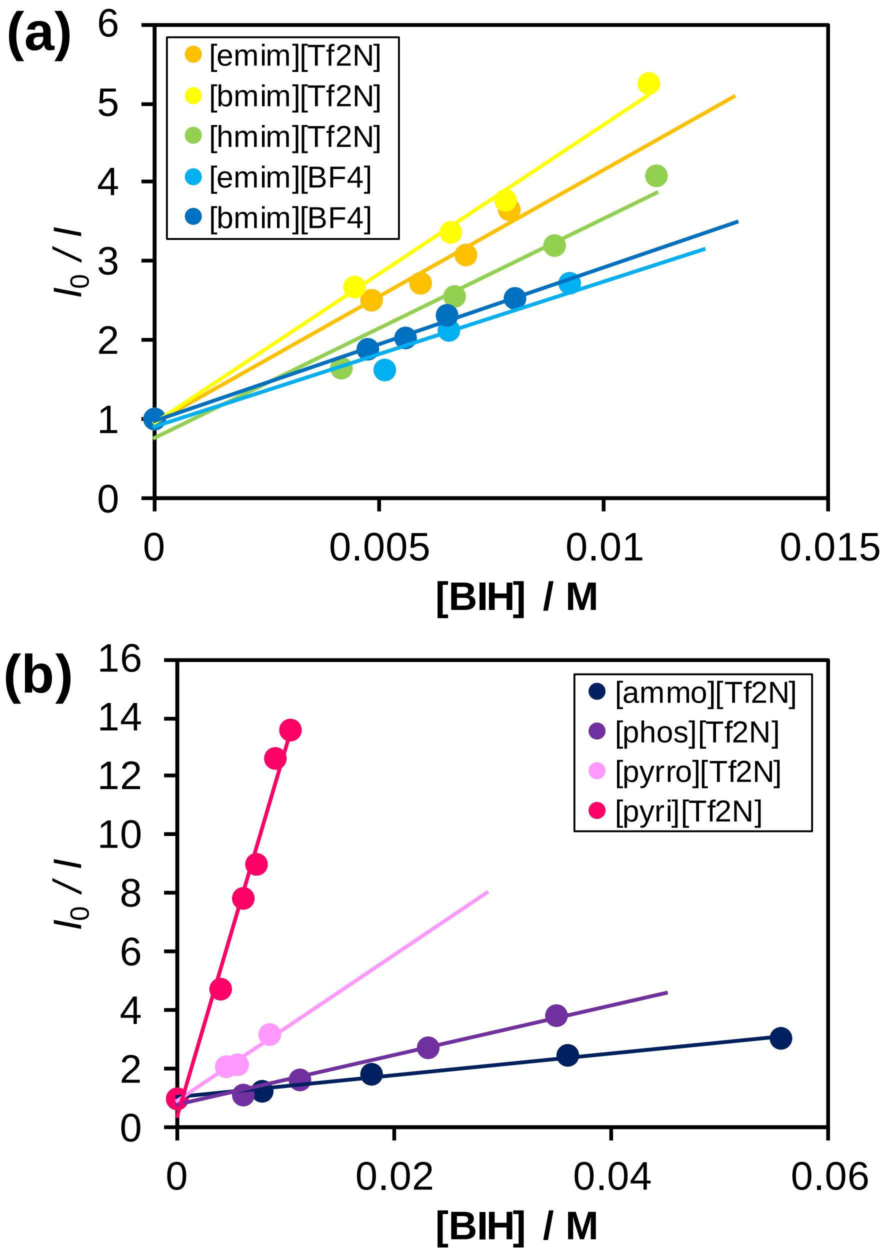

Figure S3. The Stern-Volmer plots in each of the ionic liquids using emission intensity (*I*) and the emission intensity without any BIH (I_0). The determination coefficients (R^2) of the fitting curves were larger than 0.95.

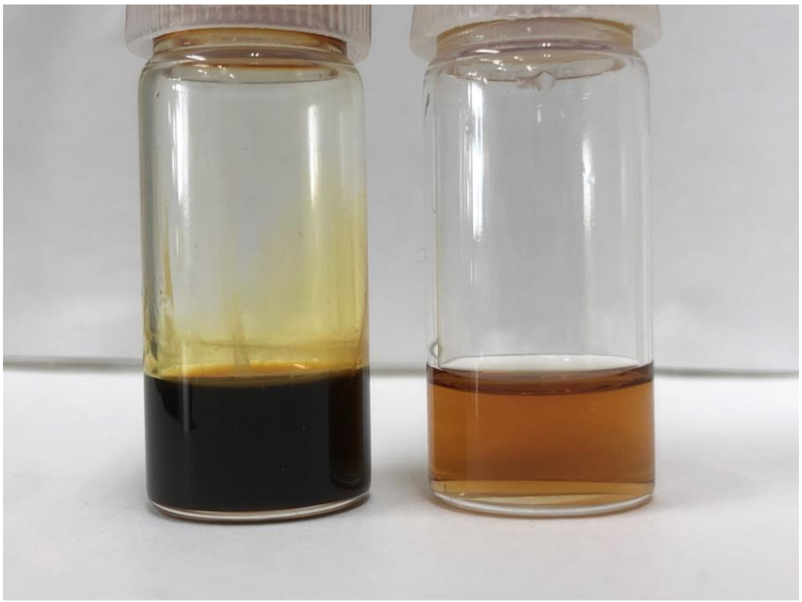

Figure S4. The [pyri][Tf_2N] (left) and [pyrro][Tf_2N] (right) solutions containing 0.1 M BIH.

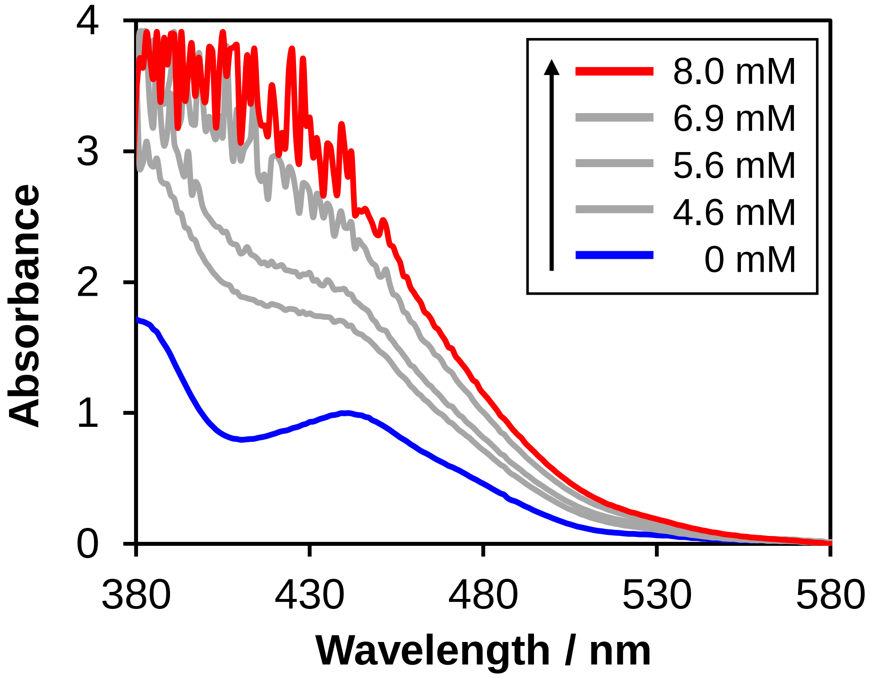

Figure S5. Absorption spectra of the [pyri][Tf_2N] solutions containing **Ir** and various amounts of BIH.

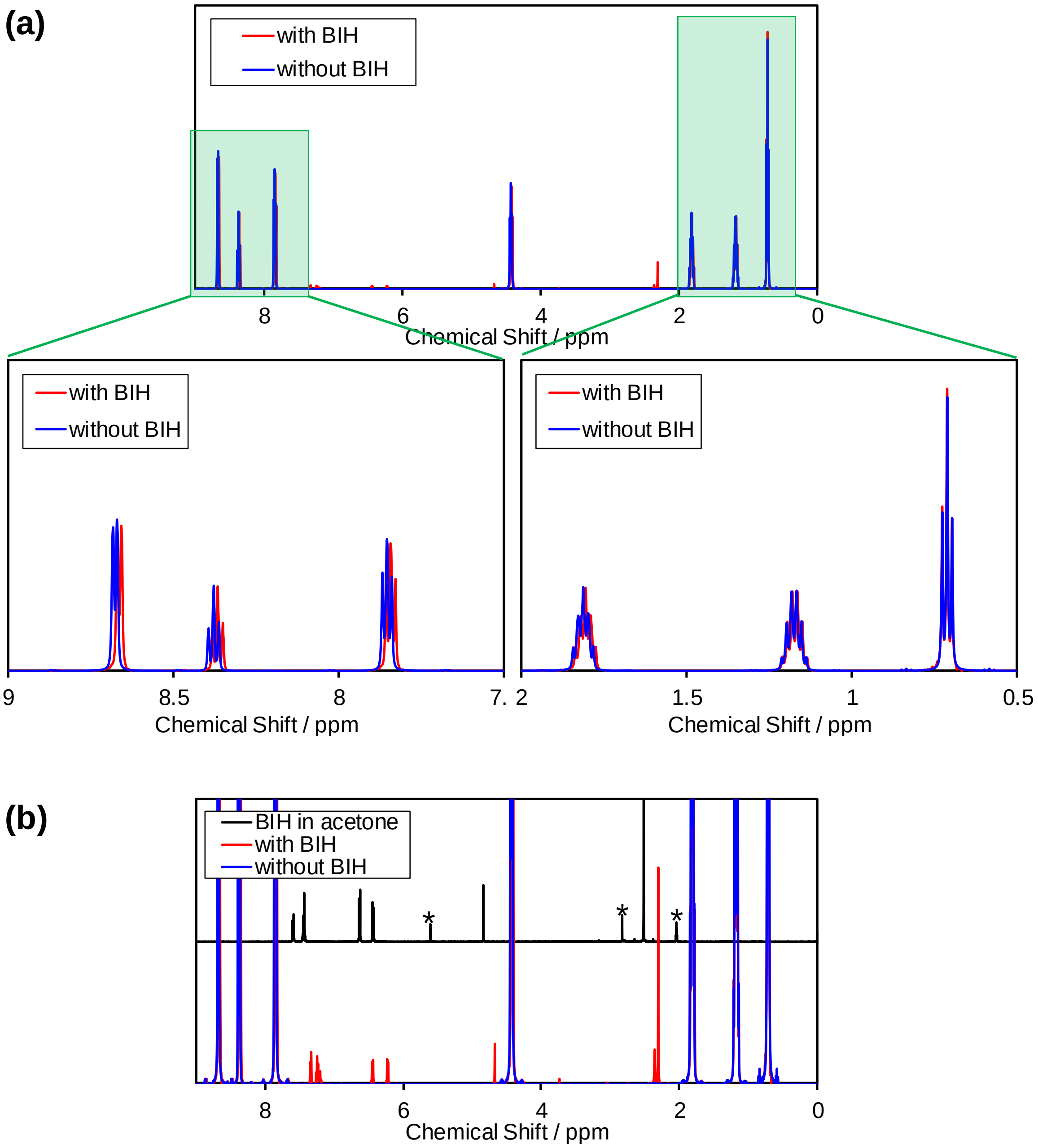

Figure S6. (a) ^{1}H NMR spectrum of [pyri][Tf$_2$N] in the absence (blue line) or in the presence (red line) of 0.1 M BIH. (b) The comparison between the spectra of BIH in [pyri][Tf$_2$N] (red line) and in acetone (black line). The asterisks (*) indicate the solvent peaks.

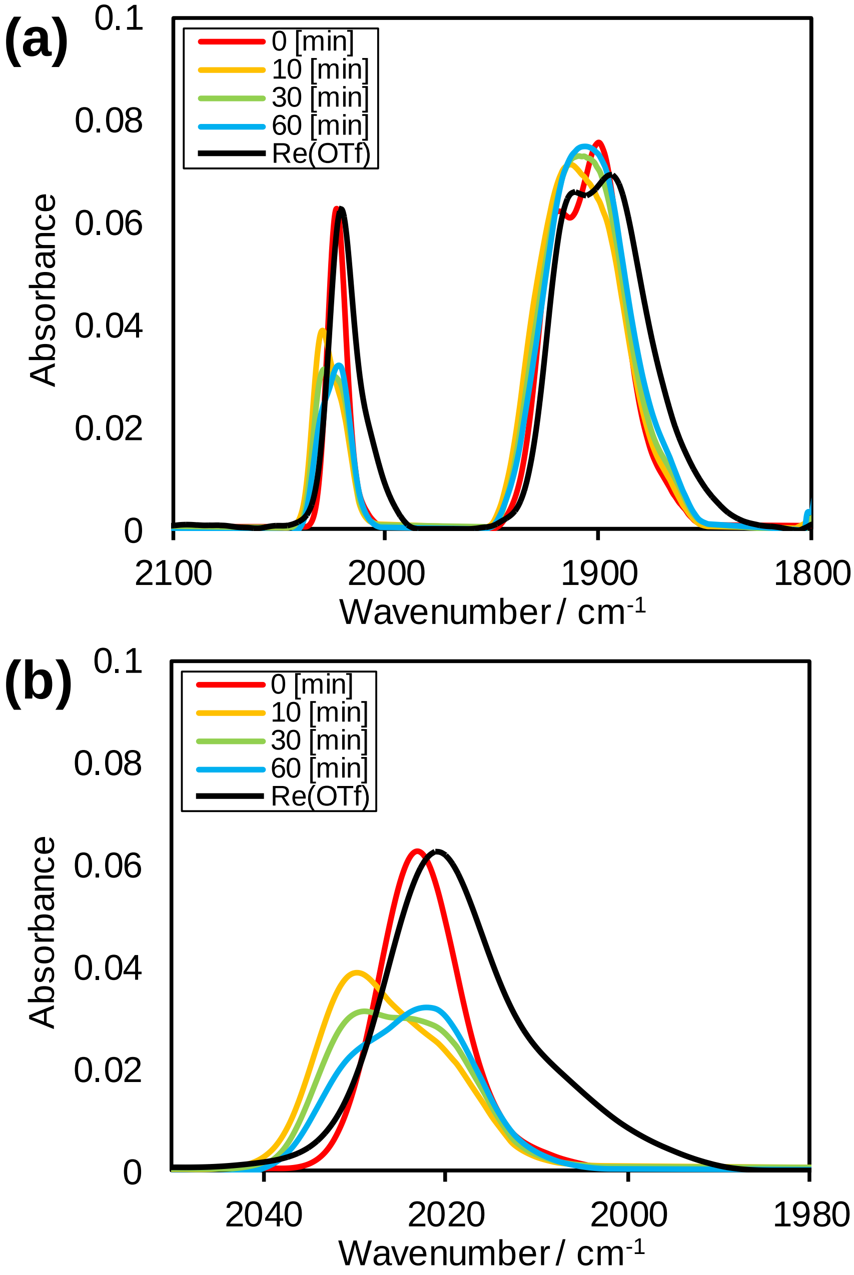

Figure S7. IR spectral changes of the [emim][OTf] solutions containing **Ir** (0.5 mM), **Re(Br)** (0.05 mM) and BIH (0.1 M) after the photocatalytic CO_2 reduction shown in Fig. 5.

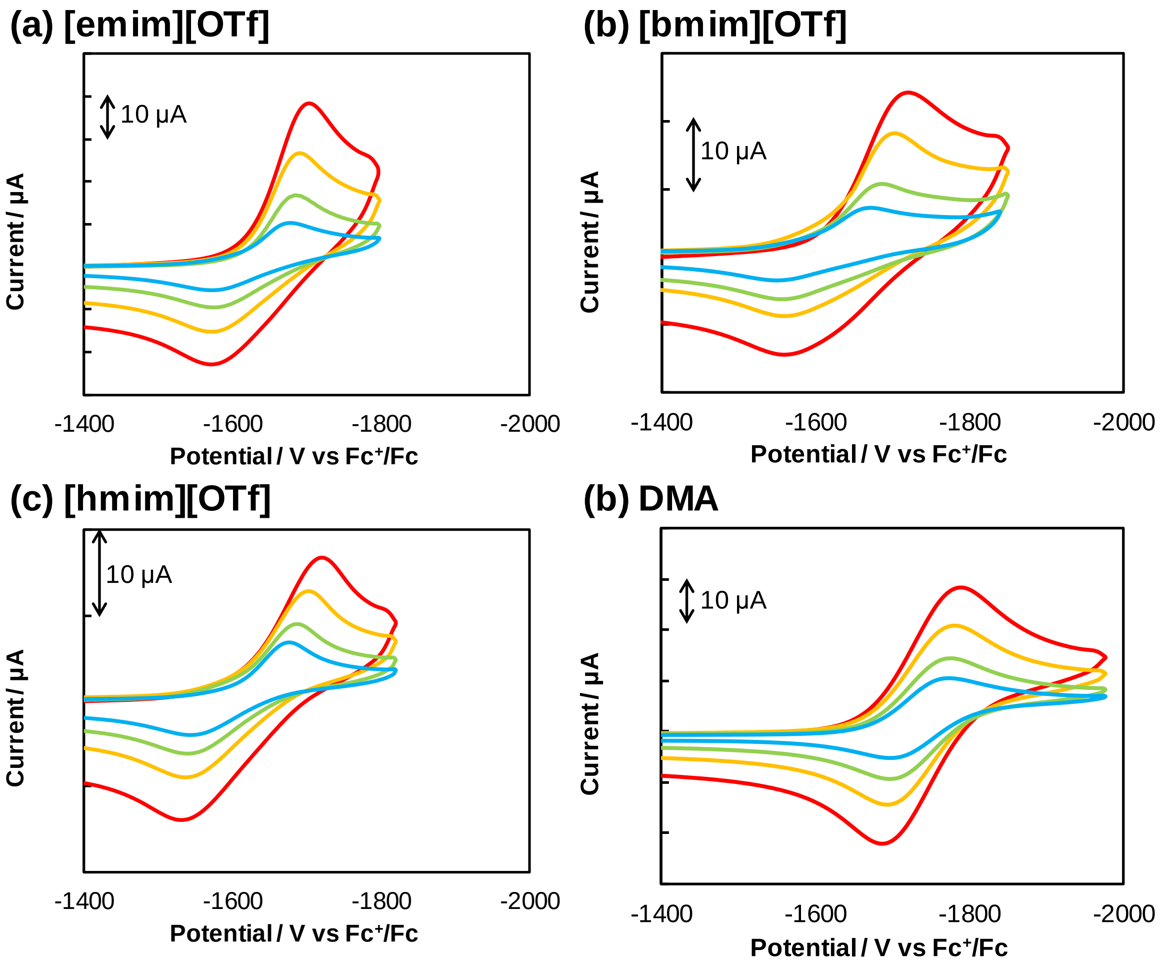

Figure S8. Cyclic voltammograms of **Re(Br)** in (a) [emim][OTf] (b) [bmim][OTf], (c) [hmim][OTf], and (d) DMA containing Bu_4NPF_6 (0.1 M) with a Ag/$AgNO_3$ (0.01 M) reference electrode using various scan rates: 50 mV/s (blue), 100 mV/s (green), 200 mV/s (orange), and 400 mV/s (red). The potential was corrected by the redox couple of ferrocene added as an internal standard. The concentration of **Re(Br)** was 5 mM for the ionic liquids and 0.5 mM for DMA solutions.

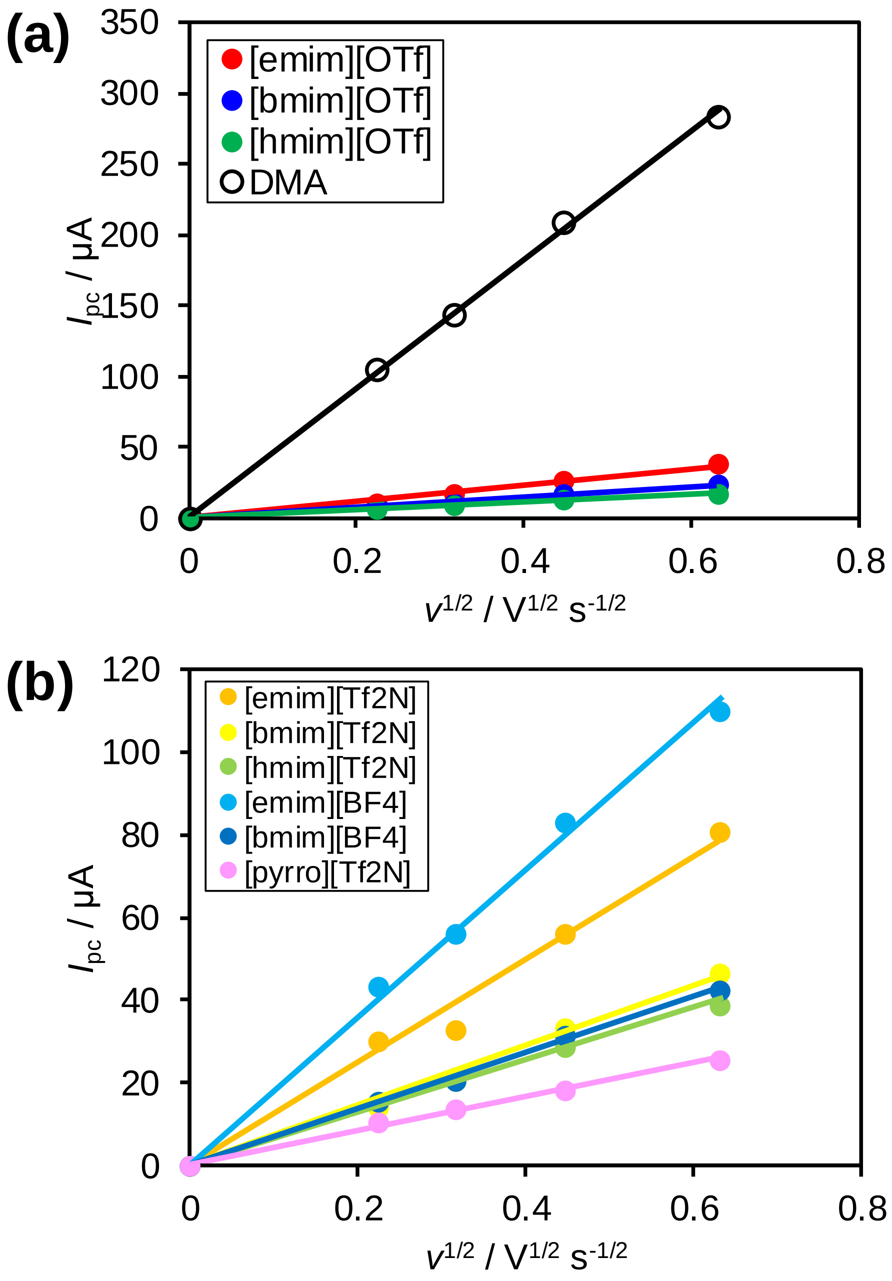

Figure S9. The relationship between i_{pc}s and $\nu^{1/2}$. The estimated diffusion coefficients in [emim][Tf_2N], [bmim][Tf_2N], [hmim][Tf_2N], [emim][BF_4], [bmim][BF_4], and [pyrro][Tf_2N] were 1.7×10^{-6} [cm^2/s], 5.7×10^{-7} [cm^2/s], 4.5×10^{-7} [cm^2/s], 3.6×10^{-6} [cm^2/s], 5.1×10^{-7} [cm^2/s], and 1.9×10^{-7} [cm^2/s], respectively. The i_{pc}s in DMA solutions were normalized by the concentration of **Re(Br)**.

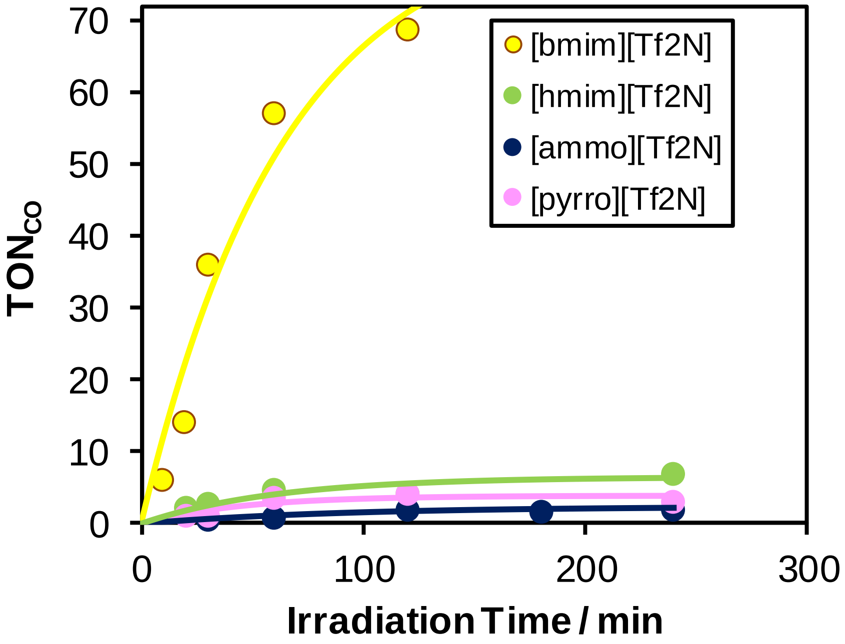

Figure S10. Time courses of the CO formation during the photocatalytic reactions ($\lambda_{ex} > 370$ nm) using 0.5 mM **Ir**, 0.05 mM **Re(Br)** and 0.1 M BIH in [bmim][Tf$_2$N] (yellow), [hmim][Tf$_2$N] (yellow-green), [ammo][Tf$_2$N] (cyan blue), or [pyrro][Tf$_2$N] (pink).

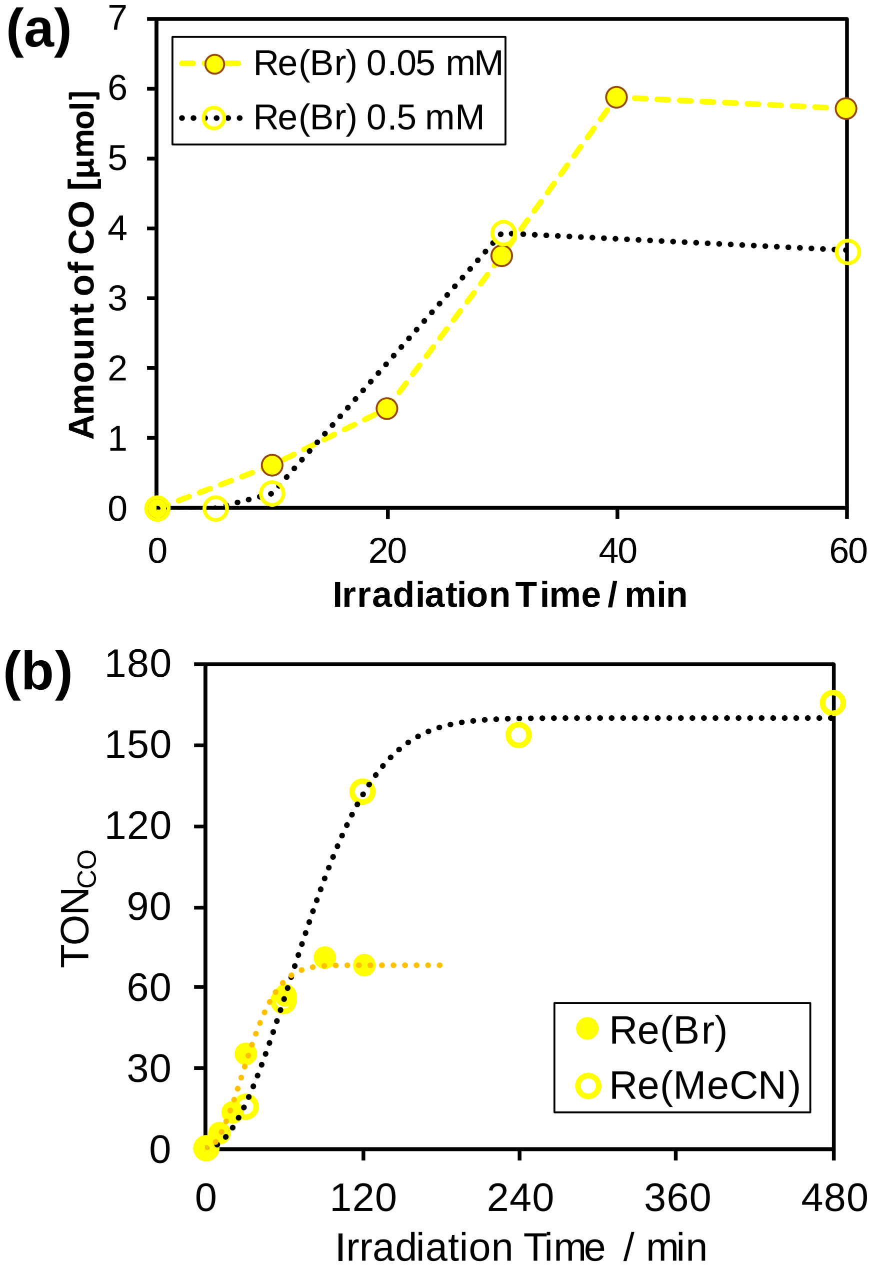

Figure S11. Time courses of the CO formation during photocatalytic reactions in [bmim][Tf$_2$N] using (a) different concentrations of **Re(Br)** or (b) different Re-catalysts.

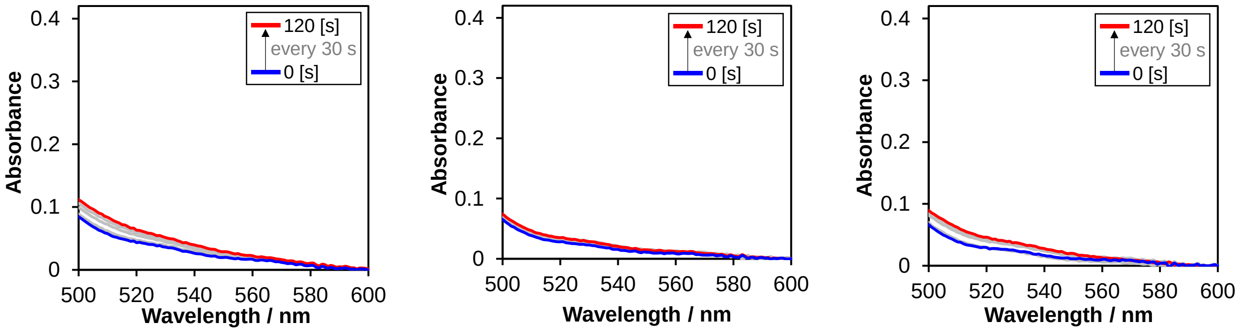
(a) [emim][Tf_2N] (b) [bmim][Tf_2N] (c) [hmim][Tf_2N]

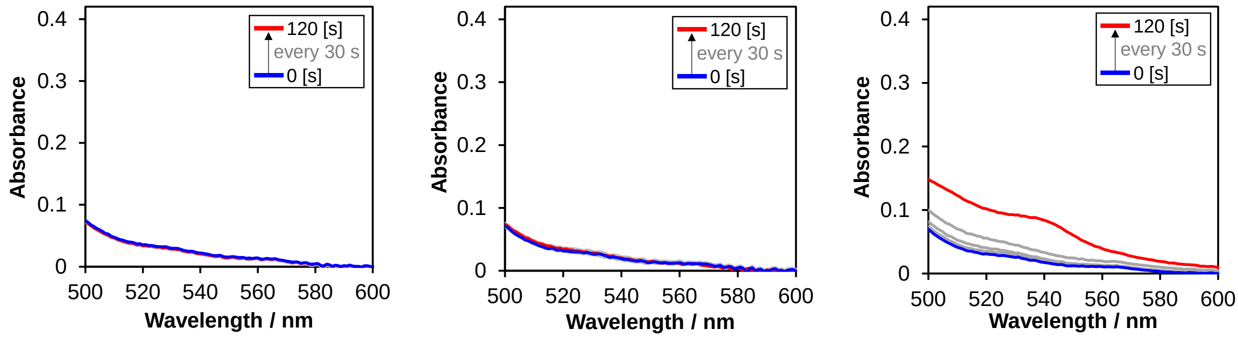
(d) [emim][BF_4] (e) [bmim][BF_4] (f) [ammo][Tf_2N]

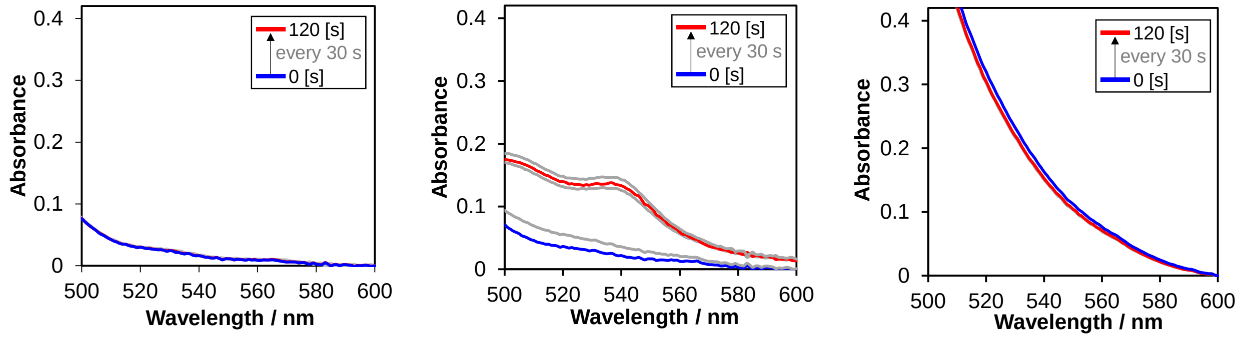
(g) [phos][Tf_2N] (i) [pyrro][Tf_2N] (h) [pyri][Tf_2N]

Figure S12. Absorption spectral changes in each of the ionic liquids containing **Ir** (0.5 mM) and BIH (0.1 M) during irradiation (λ_{ex} > 370 nm) under Ar atmosphere.

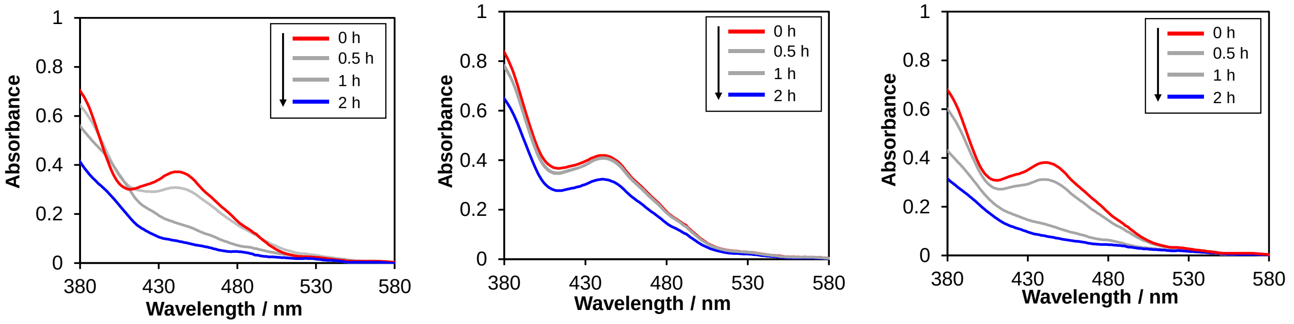

(a) [bmim][OTf] (b) [hmim][OTf] (c) [emim][Tf$_2$N]

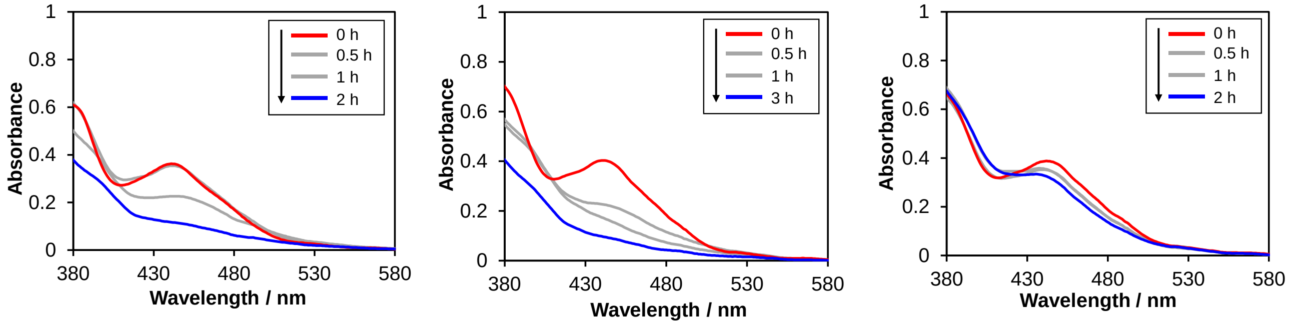

(d) [bmim][Tf$_2$N] (e) [hmim][Tf$_2$N] (f) [emim][BF$_4$]

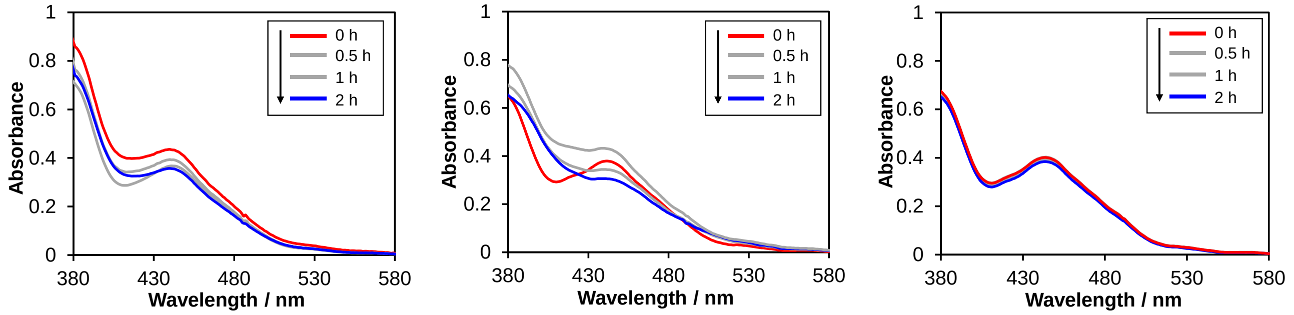

(g) [bmim][BF$_4$] (h) [ammo][Tf$_2$N] (i) [phos][Tf$_2$N]

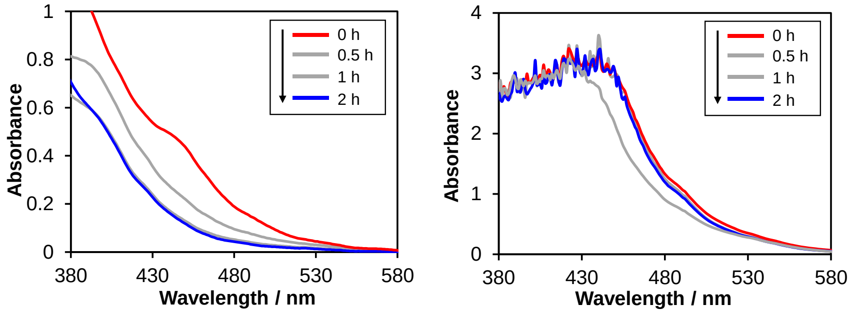

(j) [pyrro][Tf$_2$N] (k) [pyri][Tf$_2$N]

Figure S13. Absorption spectral changes of the investigated ionic-liquid solutions containing **Ir** (0.5 mM), **Re(Br)** (0.05 mM) and BIH (0.1 M) after the photo-irradiation under CO_2 atmosphere.

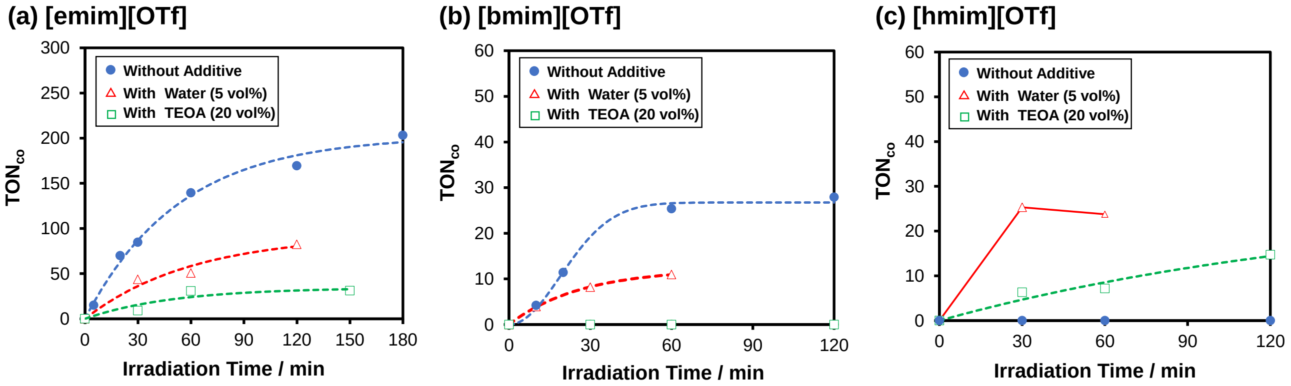

Figure S14. Time courses of the CO formation during the photocatalytic reactions ($\lambda_{ex} > 370$ nm) using 0.5 mM **Ir**, 0.05 mM **Re(Br)** and 0.1 M BIH in (a) [emim][OTf], (b) [bmim][OTf] or (c) [hmim][OTf]; without any additive (filled blue circles), with water (5 vol%, open red triangles), with TEOA (20 vol%, open green squares).

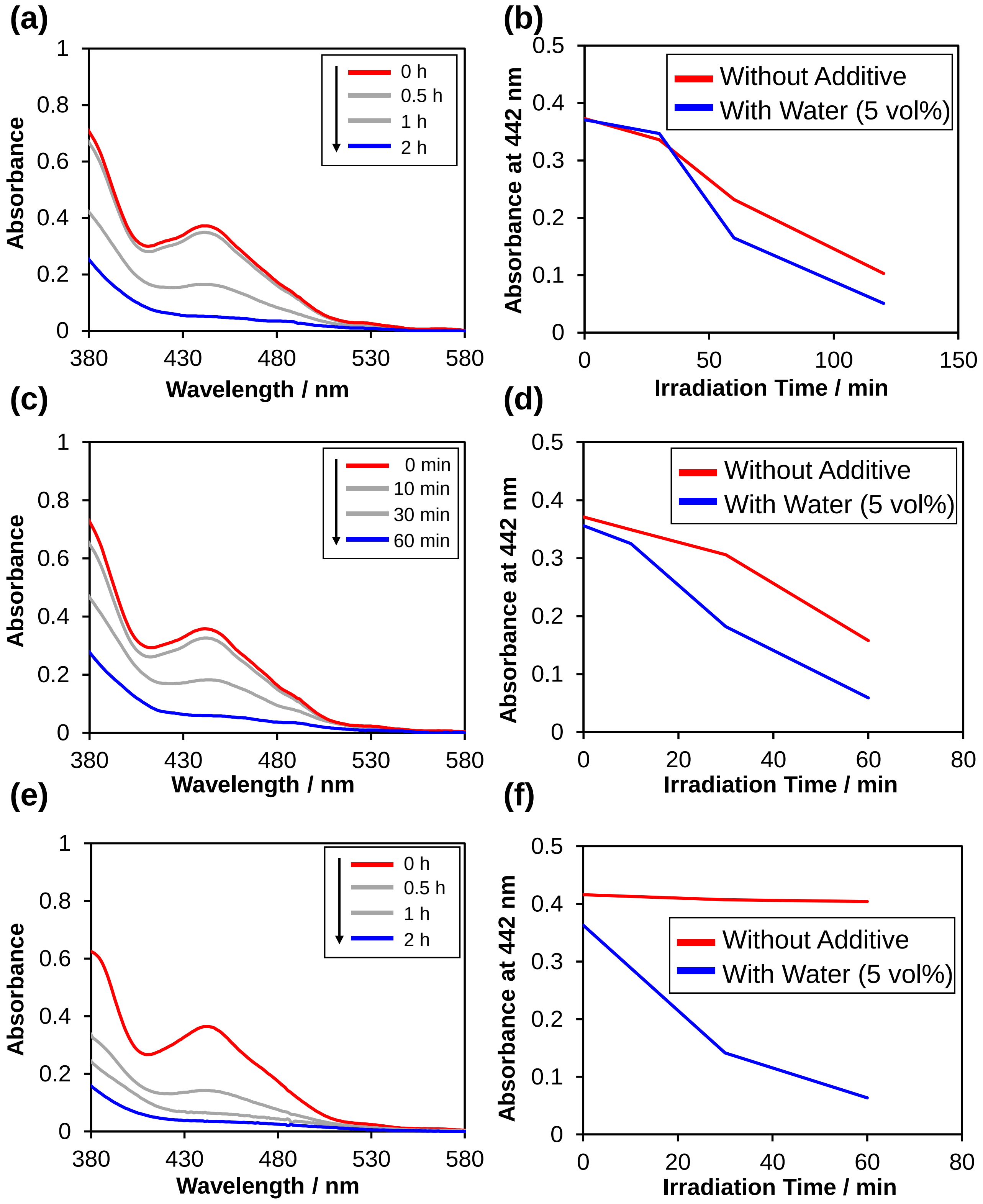

Figure S15. Absorption spectral changes of (a) the [emim][OTf] solutions, (c) the [bmim][OTf] solutions, and (e) the [hmim][OTf] solutions, containing **Ir** (0.5 mM), **Re(Br)** (0.05 mM) and BIH (0.1 M) in the presence of water of 5 vol% after the photocatalytic CO_2 reduction. Time profiles of the absorbance at 442 nm are illustrated in (b), (d), and (f), respectively.

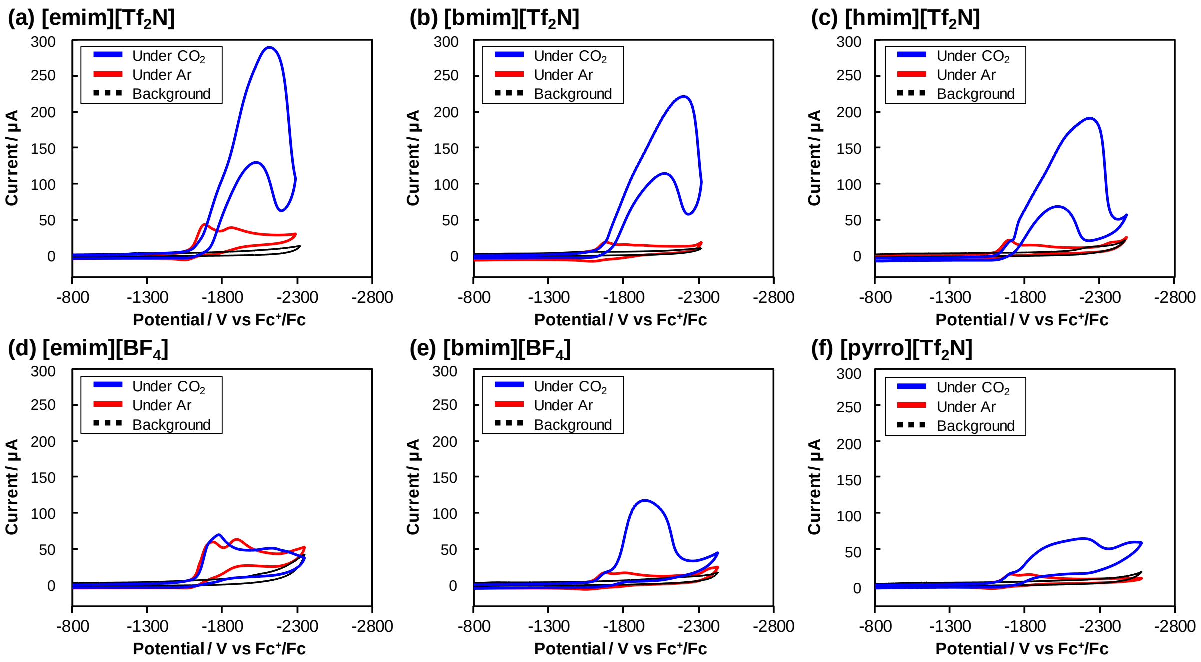

Figure S16. Cyclic voltammograms of **Re(Br)** under Ar (red line) or CO_2 atmosphere (blue line) in each of the ionic liquids with a Ag/$AgNO_3$ (0.01 M) reference electrode. The potential was corrected by the redox couple of ferrocene added as an internal standard. In the case of [ammo][Tf_2N] and [phos][Tf_2N], the reduction waves were not successfully recorded likely due to the tremendously high viscosity.

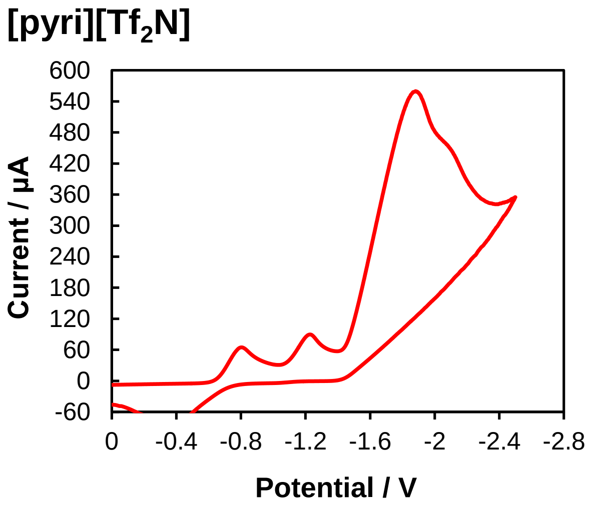

Figure S17. A cyclic voltammogram of [pyri][Tf$_2$N].